

MHD Falkner-Skan Flow with Mixed Convection and Convective Boundary Conditions

Masood KHAN, Ramzan ALI* and Azeem SHAHZAD

Department of Mathematics, Quaid-i-Azam University, Islamabad 44000, Pakistan

(*Corresponding author's e-mail: alian.qau@gmail.com)

Received: 7 June 2012, Revised: 28 July 2012, Accepted: 8 July 2013

Abstract

In this paper we investigate the simultaneous effects of thermal and concentration diffusions on a mixed convection magnetohydrodynamic (MHD) Falkner-Skan boundary layer flow through a porous medium under a convective surface boundary condition. The governing boundary layer equations are written in dimensionless form by similarity transformations. The transformed coupled nonlinear ordinary differential equations are solved analytically by using the homotopy analysis method (HAM). The effects of different parameters on the velocity, temperature and concentration fields are analyzed and discussed. Tables containing the numerical data for the local Nusselt and Sherwood numbers are also provided.

Keywords: Analytical solutions, Falkner-Skan flow, convective surface boundary condition, mixed convection

Introduction

During the past several decades, the study of magneto-hydrodynamic boundary layer flow through a porous medium with heat and mass transfer over a wedge surface has attracted considerable attention. This interest is due to several important applications such as reactive polymer flows in heterogeneous porous media, electrochemical generation of elemental bromine in porous electrode systems, manufacture of intumescent paints for fire safety applications and so forth. In their pioneering work Falkner and Skan [1] initially discussed the concept of the wedge phenomenon for two-dimensional flow. They [1] used self-similarity transformation to reduce the partial differential equation to a non-linear third order ordinary differential equation which is in fact a generalization of the Blasius boundary layer flow by considering a wedge angle for velocity field. Since then, a large number of investigations dealing with magnetohydrodynamic boundary layer flow with heat and/or mass transfer over a wedge surface have been made. In particular, Lin and Lin [2], Kuo [3], Watanabe [4], Chamkha and Khaled [5], Cheng and Lin [6], Fang and Zhang [7], Abbasbandy and Hayat [8] and Hayat *et al.* [9] studied wedge boundary layer flows with heat and/or mass transfer.

The above studies all related to the flow, heat and/or mass transfer have been made using either a constant surface temperature or a constant heat flux boundary condition. In the present investigation, we are interested in the magnetohydrodynamic wedge boundary layer flow with heat and mass transfer together with the convective surface boundary condition. The convective surface boundary condition is more general and realistic especially with respect to engineering and industrial processes material drying, transpiration cooling process and so forth. The available literature [10-15] on boundary layer flows reveals that very little work has been carried out using a convective surface boundary condition.

According to the author's best knowledge; no studies have thus far been communicated with regards to the Falkner-Skan boundary layer flow with heat and mass transfer together with mixed convection and a convective boundary condition. The objective of the present paper is therefore to investigate the simultaneous effects of thermal and concentration diffusions on a mixed convection magnetohydrodynamic

boundary layer flow through a porous medium and a convective boundary condition at the wedge surface. The problem is solved analytically using the Homotopy Analysis Method (HAM) [16-25] and the results are presented for the velocity, temperature and concentration profiles together with the local heat and mass transfer rates.

Mathematical formulation

Let us consider a two-dimensional steady, hydromagnetically coupled heat and mass transfer by mixed convection boundary layer flow of an incompressible viscous fluid of temperature T_∞ and concentration C_∞ in front of a stagnation point on a wedge plate embedded in a porous medium. Let the x -axis be taken along the direction of the wedge and the y -axis normal to it. A transverse magnetic field of strength $B(x)$ is applied parallel to the y -axis. It is assumed that the induced magnetic field, the external electric field, and the electric field due to the polarization of charges are negligible. It is also assumed that the bottom surface of the wedge plate is heated by convection from a hot fluid at temperature T_f which provides a heat transfer coefficient h . The wedge surface is maintained at a constant concentration C_w . Under the boundary layer approximations, the continuity, momentum, energy balance and concentration equations with appropriate boundary conditions can be written in as;

$$\frac{\partial u}{\partial x} + \frac{\partial v}{\partial y} = 0, \quad (1)$$

$$u \frac{\partial u}{\partial x} + v \frac{\partial u}{\partial y} = U \frac{dU}{dx} + \nu \frac{\partial^2 u}{\partial y^2} + g[\beta(T - T_\infty) + \beta^*(C - C_w)] \sin\left(\frac{\Omega}{2}\right) - \left[\frac{\sigma B^2(x)}{\rho} + \frac{\phi \nu}{k_1}\right](u - U), \quad (2)$$

$$u \frac{\partial T}{\partial x} + v \frac{\partial T}{\partial y} = \frac{k}{\rho c_p} \frac{\partial^2 T}{\partial y^2}, \quad (3)$$

$$u \frac{\partial C}{\partial x} + v \frac{\partial C}{\partial y} = D \frac{\partial^2 C}{\partial y^2}, \quad (4)$$

$$u = v = 0, \quad -k \frac{\partial T}{\partial y} = h(T_f - T), \quad C = C_w \quad \text{at } y = 0, \quad (5)$$

$$u = U(x), \quad T = T_\infty, \quad C = C_\infty \quad \text{as } y \rightarrow \infty, \quad (6)$$

where

$$U(x) = bx^r, \quad b \text{ is a positive constant and } B(x) = B_0 x^{(r-1)/2}.$$

In the above equation, u and v are the velocity components along axes x and y , respectively, r the wedge parameter, g the acceleration due to gravity, T and C are temperature and concentration respectively, β the coefficient of the volume expansion for heat transfer, β^* the coefficient of the volumetric expansion with respect to species concentration, D the molecular

diffusivity, σ the electrical conductivity, B_0 the magnetic field, Ω the wedge angle, c_p the specific heat coefficient at constant pressure and k indicates the thermal conductivity of the fluid.

We introduce the following dimensionless quantities.

$$\eta = \frac{y}{x} \sqrt{\frac{r+1}{2}} \frac{Ux}{\nu}, \quad u = Uf'(\eta), \quad v = -\frac{\nu}{x} \sqrt{\frac{r+1}{2}} \frac{Ux}{\nu} \left(f + \frac{r-1}{r+1} \eta f' \right),$$

$$\theta = \frac{T - T_\infty}{T_f - T_\infty} \text{ and } \phi = \frac{C - C_\infty}{C_w - C_\infty}.$$
(7)

The above governing problem is then reduced to;

$$\frac{d^3 f}{d\eta^3} + f \frac{d^2 f}{d\eta^2} + \frac{2r}{r+1} \left[1 - \left(\frac{df}{d\eta} \right)^2 \right] - \left[M^2 + \frac{1}{K} \right] \left(\frac{df}{d\eta} - 1 \right) + \frac{r+1}{2} \sin\left(\frac{\Omega}{2}\right) \lambda [\theta + N\phi] = 0,$$
(8)

$$\frac{1}{Pr} \frac{d^2 \theta}{d\eta^2} + f \frac{d\theta}{d\eta} = 0,$$
(9)

$$\frac{1}{Sc} \frac{d^2 \phi}{d\eta^2} + f \frac{d\phi}{d\eta} = 0,$$
(10)

$$f(\eta) = f'(\eta) = 0, \quad \theta'(\eta) = -\gamma[1 - \theta(\eta)], \quad \phi(\eta) = 1 \text{ at } \eta = 0,$$
(11)

$$f'(\eta) = 1, \quad \theta(\eta) = \phi(\eta) = 0 \text{ as } \eta \rightarrow \infty,$$
(12)

where $M^2 = 2\sigma B_0 / \rho b(1+r)$ is the magnetic parameter, $Pr = \frac{\mu c_p}{k}$ the Prandtl number, $\lambda = 2g\beta(T_w - T_\infty)x / (r+1)U^2$ the mixed convection parameter, $N = \frac{\beta^*(C_w - C_\infty)}{\beta(T_w - T_\infty)}$ the buoyancy ratio, $Sc = \frac{\nu}{D}$ the Schmidt number, $K = \frac{(r+1)k^*U}{2\phi_1 x \nu}$ the permeability parameter and;

$$\gamma = \frac{h_f}{k} \sqrt{\frac{2}{r+1}} \sqrt{\nu x / U}.$$
(13)

For an energy equation to have a similarity solution, the quantity γ must be independent of x . Consequently, the heat transfer coefficient h_f is proportional to $x^{-1/2}$ and we assume;

$$h_f = \sqrt{\frac{r+1}{2}} c x^{-1/2},$$
(14)

and get;

$$\gamma = \frac{c}{k} \sqrt{\nu/U}, \quad (15)$$

as the Biot number with c as arbitrary constant. We note that when $\gamma \rightarrow \infty$, the present problem reduces to the classical boundary layer flow on the wedge with constant surface temperature.

The local Nusselt number Nu_x and local Sherwood number Sh_x may be found in terms of the dimensionless temperature at the wedge surface, $\theta'(0)$, and the dimensionless concentration at the wedge surface, $\phi'(0)$, respectively, that is;

$$Nu_x = Re_x^{-1/2} Nu = -\theta'(0), \quad (16)$$

$$Sh_x = Re_x^{-1/2} Sh = -\phi'(0), \quad (17)$$

where $Nu = \frac{q_w x}{k(T_w - T_\infty)}$, $Sh = \frac{q_m x}{D(\phi_w - \phi_\infty)}$ and $Re_x = \sqrt{\frac{m+1}{2}} \frac{u_w x}{\nu}$ with q_w as the surface heat flux and q_m the surface mass flux.

The HAM solutions

According to Eqs. (8) - (10) and the boundary conditions (11) - (12), the solutions for the velocity, temperature and concentration fields can be expressed in the form of the following homotopy series

$$f(\eta) = \sum_{i=0}^{\infty} \sum_{j=0}^{\infty} a_{i,j} \eta^i \exp(-j\eta), \quad (18)$$

$$\theta(\eta) = \sum_{i=0}^{\infty} \sum_{j=0}^{\infty} b_{i,j} \eta^i \exp(-j\eta), \quad (19)$$

$$\phi(\eta) = \sum_{i=0}^{\infty} \sum_{j=0}^{\infty} c_{i,j} \eta^i \exp(-j\eta), \quad (20)$$

where $a_{i,j}$, $b_{i,j}$ and $c_{i,j}$ are coefficients. Here we choose the initial guesses and auxiliary linear operators in the following forms;

$$f_0(\eta) = \eta - \frac{(1 - e^{-2\eta})}{2}, \quad (21)$$

$$\theta_0(\eta) = \frac{\gamma e^{-\eta}}{1 + \gamma}, \quad (22)$$

$$\phi_0(\eta) = e^{-\eta}, \quad (23)$$

$$\mathfrak{L}_f[\hat{f}(\eta, p)] = \frac{\partial^3 \hat{f}(\eta, p)}{\partial \eta^3} - \frac{\partial \hat{f}(\eta, p)}{\partial \eta}, \quad (24)$$

$$\mathfrak{L}_\theta[\hat{\theta}(\eta, p)] = \frac{\partial^2 \hat{\theta}(\eta, p)}{\partial \eta^2} - \hat{\theta}(\eta, p), \quad (25)$$

$$\mathfrak{L}_\phi[\hat{\phi}(\eta, p)] = \frac{\partial^2 \hat{\phi}(\eta, p)}{\partial \eta^2} - \hat{\phi}(\eta, p), \quad (26)$$

Making use of the above definitions, we construct the zero-order deformation problem as follows;

$$(1-p)\mathfrak{L}_f[\hat{f}(\eta, p) - f_0(\eta)] = p\hbar_f N_f[\hat{\theta}(\eta, p), \hat{\phi}(\eta, p), \hat{f}(\eta, p)], \quad (27)$$

$$(1-p)\mathfrak{L}_\theta[\hat{\theta}(\eta, p) - \theta_0(\eta)] = p\hbar_\theta N_\theta[\hat{\theta}(\eta, p), \hat{f}(\eta, p)], \quad (28)$$

$$(1-p)\mathfrak{L}_\phi[\hat{\phi}(\eta, p) - \phi_0(\eta)] = p\hbar_\phi N_\phi[\hat{\phi}(\eta, p), \hat{f}(\eta, p)], \quad (29)$$

$$\hat{f}(\eta, p) = \hat{f}'(\eta, p) = 0, \hat{\phi}(\eta, p) = 1 \text{ and } \hat{\theta}(\eta, p) = -\gamma[1 - \hat{\theta}(\eta, p)] \text{ at } \eta = 0, \quad (30)$$

$$\hat{f}'(\eta, p) = \hat{\theta}(\eta, p) = \hat{\phi}(\eta, p) = 0 \quad \text{as} \quad \eta \rightarrow \infty, \quad (31)$$

where

$$\begin{aligned} N_f[\hat{f}(\eta, p)] = & \hat{f}'''(\eta, p) + \hat{f}(\eta, p)\hat{f}''(\eta, p) - \left(\frac{2r}{r+1}\right)\hat{f}'(\eta, p)\hat{f}'(\eta, p) \\ & - M^2 \hat{f}'(\eta, p) + \frac{r+1}{2}\lambda[\hat{\theta}(\eta, p) + N\hat{\phi}(\eta, p)]\sin\left(\frac{\Omega}{2}\right) - \frac{1}{K}\hat{f}'(\eta, p) + \left(M^2 + \frac{2r}{r+1} + \frac{1}{K}\right), \end{aligned} \quad (32)$$

$$N_\theta[\hat{\theta}(\eta, p), \hat{f}(\eta, p)] = \frac{1}{\text{Pr}}\hat{\theta}''(\eta, p) + (\hat{f}(\eta, p)\hat{\theta}'(\eta, p)) \quad (33)$$

$$N_\phi[\hat{\phi}(\eta, p), \hat{f}(\eta, p)] = \frac{1}{Sc}\hat{\phi}''(\eta, p) + (\hat{f}(\eta, p)\hat{\phi}'(\eta, p)) \quad (34)$$

where $p \in [0, 1]$ is an embedding parameter and \hbar_f , \hbar_θ and \hbar_ϕ are the non-zero convergence control parameters.

Note that;

$$\hat{f}(\eta, 0) = f_0(\eta), \quad \hat{\theta}(\eta, 0) = \theta_0(\eta) \quad \text{and} \quad \hat{\phi}(\eta, p) = \phi_0(\eta), \quad (35)$$

$$\hat{f}(\eta, 1) = f(\eta), \quad \hat{\theta}(\eta, 1) = \theta(\eta) \quad \text{and} \quad \hat{\phi}(\eta, 1) = \phi(\eta) \quad \text{as} \quad \eta \rightarrow \infty, \quad (36)$$

When the embedding parameter p , increases from 0 to 1. Then in consequences the parameters $\hat{f}(\eta; p)$, $\hat{\theta}(\eta; p)$ and $\hat{\phi}(\eta; p)$ vary from initial solutions $f_0(\eta)$, $\theta_0(\eta)$ and $\phi_0(\eta)$ to the final solutions $f(\eta)$, $\theta(\eta)$ and $\phi(\eta)$, respectively. Using Taylor's theorem, we can write;

$$\hat{f}(\eta; p) = f_0(\eta) + \sum_{m=1}^{\infty} f_m p^m, \quad (37)$$

$$\hat{\theta}(\eta; p) = \theta_0(\eta) + \sum_{m=1}^{\infty} \theta_m p^m, \quad (38)$$

$$\hat{\phi}(\eta; p) = \phi_0(\eta) + \sum_{m=1}^{\infty} \phi_m p^m, \quad (39)$$

where

$$f_m(\eta) = \frac{1}{m!} \left. \frac{\partial^m \hat{f}(\eta, p)}{\partial p^m} \right|_{p=0}, \quad (40)$$

$$\theta_m(\eta) = \frac{1}{m!} \left. \frac{\partial^m \hat{\theta}(\eta, p)}{\partial p^m} \right|_{p=0} \quad (41)$$

$$\phi_m(\eta) = \frac{1}{m!} \left. \frac{\partial^m \hat{\phi}(\eta, p)}{\partial p^m} \right|_{p=0}. \quad (42)$$

The convergence of the series (37), (38) and (39) is strongly dependent upon \hbar_f , \hbar_θ and \hbar_ϕ . Assume that \hbar_f , \hbar_θ and \hbar_ϕ are chosen so that the above series are convergent at $p = 1$. From Eqs. (37), (38) and (39) we have;

$$f(\eta) = f_0(\eta) + \sum_{m=1}^{\infty} f_m(\eta), \quad (43)$$

$$\theta(\eta) = \theta_0(\eta) + \sum_{m=1}^{\infty} \theta_m(\eta), \quad (44)$$

$$\phi(\eta) = \phi_0(\eta) + \sum_{m=1}^{\infty} \phi_m(\eta). \quad (45)$$

Differentiating the zero-order deformation problems m -times with respect to p , then dividing them by $m!$ and finally setting $p = 0$, we obtain the following m th-order deformation problems.

$$\mathcal{L}_f[f_m(\eta) - \chi_m f_{m-1}(\eta)] = \hbar_f R_m^f(\eta), \quad (46)$$

$$\mathcal{L}_\theta[\theta_m(\eta) - \chi_m \theta_{m-1}(\eta)] = \hbar_\theta R_m^\theta(\eta), \quad (47)$$

$$\mathcal{L}_\phi[\phi_m(\eta) - \chi_m \phi_{m-1}(\eta)] = \hbar_\phi R_m^\phi(\eta), \quad (48)$$

$$f_m'(\eta) = f_m''(\eta) = 0, \quad \theta_m'(\eta) = \gamma \theta_m(\eta), \quad \phi_m(\eta) = 0 \quad \text{at } \eta = 0, \quad (49)$$

$$f_m'(\eta) = \theta_m(\eta) = \phi_m(\eta) = 0 \quad \text{as } \eta \rightarrow \infty, \quad (50)$$

where

$$R_m^f(\eta) = f_{m-1}''' + \sum_{k=0}^{m-1} f_{m-1-k}' f_k'' - \frac{2r}{r+1} \sum_{k=0}^{m-1} f_{m-1-k}' f_k' - M^2 f_{m-1}' + \frac{r+1}{2} \lambda \sin\left(\frac{\Omega}{2}\right) [\theta_{m-1} + N \phi_{m-1}] \quad (51)$$

$$- \frac{1}{K} f_{m-1}' + \left(M^2 + \frac{2r}{r+1} + \frac{1}{K} \right) (1 - \chi_m),$$

$$R_m^\theta(\eta) = \theta_{m-1}'' + \text{Pr} \sum_{k=0}^{m-1} \theta_{m-1-k}' f_k, \quad (52)$$

$$R_m^\phi(\eta) = \phi_{m-1}'' + \text{Sc} \sum_{k=0}^{m-1} \phi_{m-1-k}' f_k, \quad (53)$$

and

$$\chi_m = \begin{cases} 0; & m > 1 \\ 1; & m \leq 1, \end{cases} \quad (54)$$

The linear non-homogeneous problems (46) - (50) can be solved by using any symbolic computational software like MATHEMATICA in the order $m = 1, 2, 3 \dots$.

Convergence of the homotopy solution

Note that in the HAM, by means of the \hbar - curve, it is straightforward to choose an appropriate range for \hbar which ensures the convergence of the solution series. To investigate the influence of \hbar_f , \hbar_θ and \hbar_ϕ on $f''(0)$, $\theta'(0)$ and $\phi'(0)$, respectively, we plotted the \hbar - curves in **Figure 1** for the range of admissible values of these parameters. From this figure, it is noticed that the admissible range of the convergence parameters \hbar_f , \hbar_θ and \hbar_ϕ are $-1.75 \leq h_f \leq -0.5$, $-1.75 \leq h_\theta \leq -0.5$, and $-1.9 \leq h_\phi \leq -0.3$, respectively.

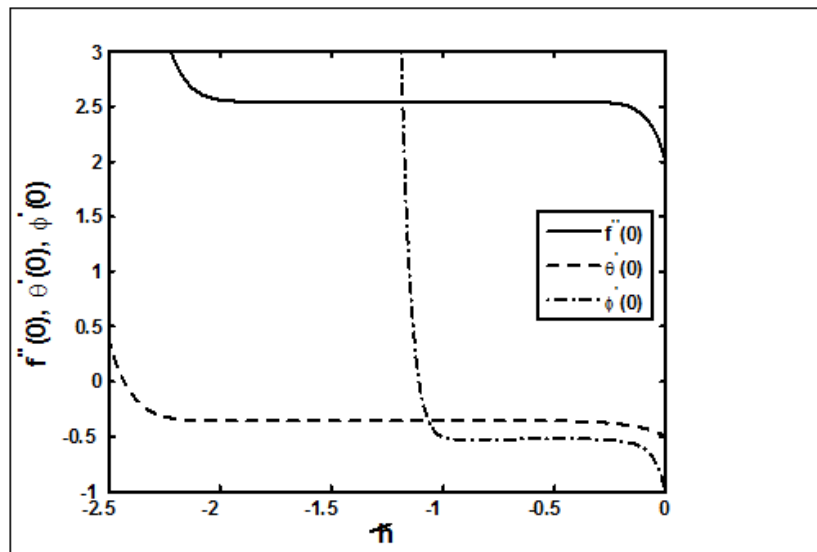


Figure 1 The h -curves of $f''(0)$, $\theta'(0)$ and $\phi'(0)$ for the 15th-order approximation for $Sc = 0.62$, $\Omega = \gamma = K = N = M = 1$, $\lambda = 2$ and $Pr = 0.71$.

Results and discussion

The system of governing Eqs. (8) - (10) subject to the boundary conditions (11) and (12) have been solved analytically via HAM. The graphical results are given to carry out a parametric study showing influences of the non-dimensional parameters on the velocity, temperature and concentration profiles.

The effects of the magnetic parameter M , and buoyancy ratio N on the velocity profile $f'(\eta)$ are displayed in **Figures 2** and **3**, respectively. These figures depict that an increases in the magnetic parameter M and buoyancy ratio N will decrease the velocity boundary layer thickness moreover, an increase in these parameters decreases the velocity gradient of the fluid in the boundary layer. **Figure 4** shows the effects of the mixed convection parameter λ on the velocity profile $f'(\eta)$. It is observed that the velocity and the boundary layer thickness increases with an increase in the mixed convection parameter λ .

The effects of the Prandtl number Pr and mixed convection parameter λ on the temperature profile $\theta(\eta)$ are shown in **Figures 5** and **6**, respectively. It is observed that the temperature decreases with an increase in the Prandtl number Pr and mixed convection parameter λ . This reduction in the velocity as well as the boundary layer thickness is greater for the Prandtl number Pr when compared with the mixed convection parameter λ .

Figure 7 indicates the effects of varying the Biot number γ on the temperature profile $\theta(\eta)$. Note that the Biot number γ is the ratio of the internal thermal resistance of a solid to the boundary layer thermal resistance. When $\gamma = 0$ the bottom side of the wedge plate with the hot fluid is totally insulated and as a result no convective heat transfer to the cold fluid above the wedge plate takes place. From **Figure 7**, it is clear that as the Biot number γ increases, the temperature θ increases significantly. This is due to the fact that as the convection Biot number increases, the wedge thermal resistance reduces.

In **Figure 8**, the concentration profile ϕ are plotted for different values of Schmidt number Sc . It

is observed that increasing the Schmidt number Sc , the species concentration drops more rapidly as the thickness of the concentration boundary layer decreases. This is due to the fact that an increase in Sc implies a decrease in the molecular diffusivity D . The dependence of the concentration profile on the mixed convection parameter λ is illustrated in **Figure 9**. It is noticed that increasing the values of λ results in a decrease in the concentration boundary layer thickness.

The quantities $-\theta'(0)$ and $-\phi'(0)$ are the measures of the local heat and mass transfer rates, respectively. The values of these quantities are recorded in **Table 1** for different values of the governing parameters. We observe that local heat transfer rate increases as Pr , λ and γ increases, but decreases when Sc increases. Further, it can be seen from **Table 1** that the effects of the increasing values of Sc , λ and γ lead to an increase in the mass transfer rate while a decrease can be seen by increasing Pr .

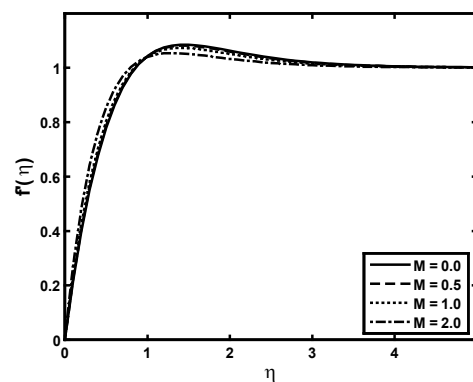


Figure 2 The effects of the magnetic parameter, M on the velocity profile $f'(\eta)$ when $Sc = 0.62$, $r = K = N = \Omega = 1$, $\lambda = 2$ and $Pr = 0.71$.

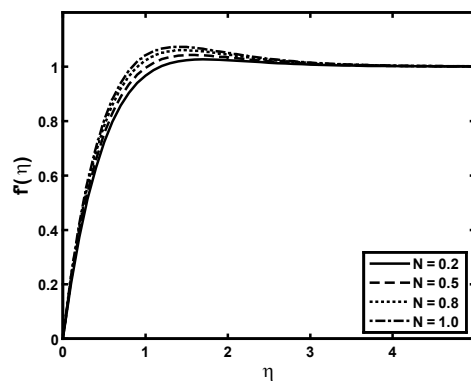


Figure 3 The effects of the buoyancy ratio N on the velocity profile $f'(\eta)$ when $Sc = 0.62$, $r = K = \lambda = M = \Omega = 1$ and $Pr = 0.71$.

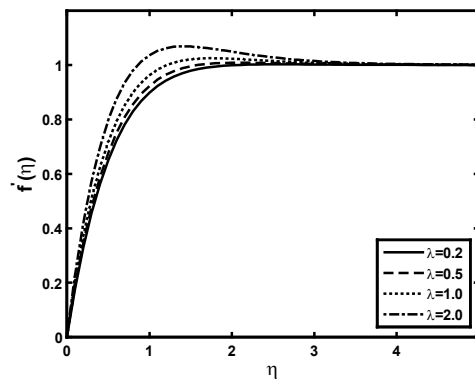


Figure 4 The effects of the convection parameter λ on the velocity profile $f'(\eta)$ when $Sc = 0.62$, $r = K = N = M = \Omega = 1$ and $Pr = 0.71$.

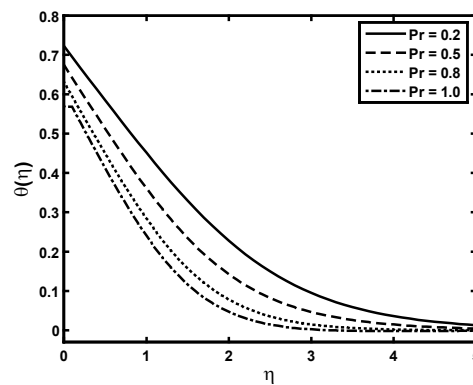


Figure 5 The effects of the Prandtl number Pr on the temperature profile $\theta(\eta)$ when $\lambda = 2$, $\gamma = r = K = N = M = \Omega = 1$ and $Sc = 0.62$.

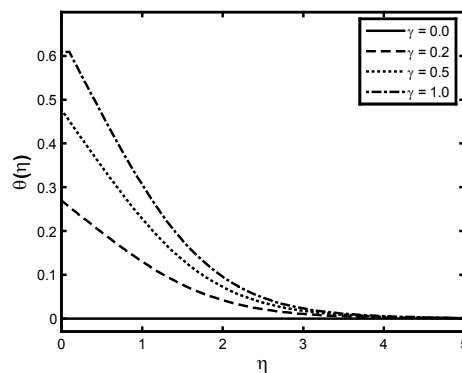


Figure 6 The effects of the Biot number γ on the temperature profile $\theta(\eta)$ when $Sc = 0.62$, $\lambda = 2$, $r = K = N = M = \Omega = 1$ and $Pr = 0.71$.

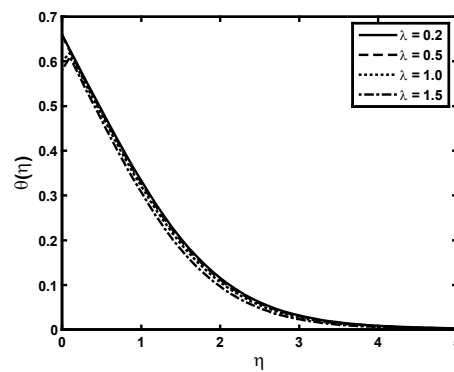


Figure 7 The effects of the mixed convection parameter λ on the temperature profile $\theta(\eta)$ when $Pr = 0.71$, $\gamma = r = K = N = M = \Omega = 1$ and $Sc = 0.62$.

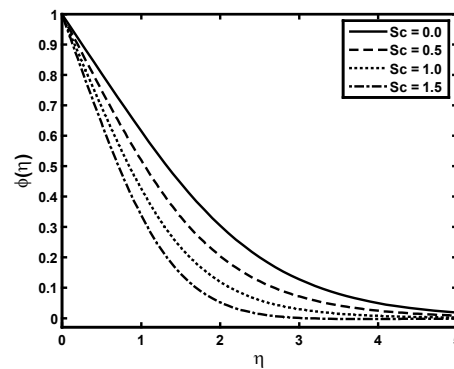


Figure 8 The effects of the mixed Schmidt number Sc on the concentration profile $\phi(\eta)$ when $\lambda = 2$, $\gamma = r = K = N = M = \Omega = 1$ and $Pr = 0.71$.

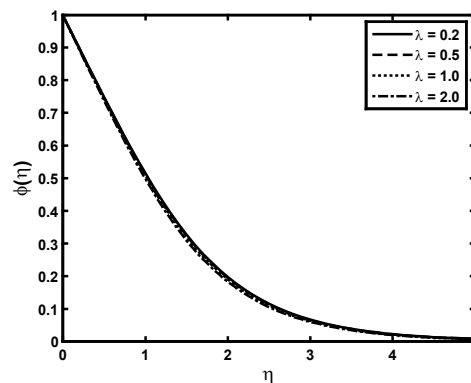


Figure 9 The effects of the mixed convection parameter λ on the concentration profile $\phi(\eta)$ when $Sc = 0.62$, $\gamma = r = K = N = M = \Omega = 1$ and $Pr = 0.71$.

Table 1 The effects of the local Nusselt number Nu_x and local Sherwood number Sh_x for several sets of the physical parameters with $Sc = 0.62$, $Pr = 0.71$, $\lambda = 2$, $\gamma = 1.0$

Sc	Pr	λ	γ	$-\theta'(0)$	$-\phi'(0)$
0.0				0.356579	0.391310
0.5				0.355646	0.502019
1.0				0.354733	0.615596
1.5				0.353854	0.728660
	0.2			0.277311	0.531372
	0.5			0.325005	0.530023
	0.8			0.36757	0.528785
	1.0			0.40246	0.528030
		0.2		0.340120	0.506907
		0.5		0.342699	0.510582
		1.0		0.346874	0.516590
		2.0		0.35479	0.528199
			0.0	0.00000	0.519689
			0.5	0.261203	0.526678
			1.0	0.355424	0.529143
			1.5	0.404431	0.530408

Conclusions

In the present paper, we have studied double-diffusive convection from a wedge plate embedded in a porous medium under convective boundary conditions. The bottom surface of the wedge plate is heated by convection from a hot fluid while the cold fluid above the wedge plate is assumed to be viscous and electrically conducting under the influence of a magnetic field. Similarity transformation was used to reduce the partial differential equations into ordinary differential equations and then solved analytically for the velocity, temperature and concentration distributions for different values of the pertinent parameters using the HAM. A table containing numerical data showing the effects of various physical parameters on the local Nusselt number (wall heat transfer rate) and local Sherwood number (wall mass transfer rate) is also provided. Our results reveal that the temperature increases significantly with an increase in the convective heat transfer parameter, that is, the Biot number γ .

Acknowledgement

The authors of the manuscript are indebted to the anonymous referees for their valuable comments.

References

- [1] AC Falkner and SW Skan. Some approximate solutions of the boundary layer equations. *Phil. Mag.* 1931; **12**, 865-96.
- [2] HT Lin and LK Lin. Similarity solution for laminar forced convection heat transfer from wedge to fluids of any Prandtl number. *Int. J. Heat Mass Tran.* 1987; **18**, 1111-8.
- [3] BL Kuo. Heat transfer analysis for the Falkner-Skan wedge flow by the differential transform method. *Int. J. Heat Mass Tran.* 2005; **48**, 5036-46.
- [4] T Watanabe. Thermal boundary layer over a wedge with uniform suction or injection in forced flow. *Acta Mech.* 1990; **83**, 119-26.
- [5] AJ Chamkha and ARA Khaled. Similarity solutions for hydro-magnetic simultaneous heat and mass transfer. *Heat Mass Tran.* 2001; **37**, 117-23.
- [6] WT Cheng and HT Lin. Non-similarity solution and correlation of transient heat transfer in laminar boundary layer over a wedge. *Int. J. Eng. Sci.* 2002; **40**, 531-48.
- [7] T Fang and J Zhang. An exact analytical solution of the Falkner-Skan equation with mass transfer and wall stretching. *Int. J. Nonlinear Mech.* 2008; **43**, 1000-6.
- [8] S Abbasbandy and T Hayat. Solution of the MHD Falkner-Skan flow by homotopy analysis method. *Commun. Nonlinear Sci. Numer. Simulat.* 2009; **14**, 3591-8.
- [9] T Hayat, M Hussain, S Nadeem and S Mesloub. Falkner-Skan wedge flow of a power law fluid with mixed convection and porous medium. *Comput. Fluid.* 2011; **49**, 22-8.
- [10] A Aziz. A similarity solution for laminar thermal boundary layer flow over a flat plate with a convective surface boundary condition. *Commun. Nonlinear Sci. Numer. Simulat.* 2009; **14**, 1064-8.
- [11] OD Makinde and A Aziz. MHD mixed convection from a vertical plate embedded in a porous medium with a convective boundary condition. *Int. J. Therm. Sci.* 2010; **49**, 1813-20.
- [12] S Yao, T Fang and Y Zhong. Heat transfer of a generalized stretching/shrinking wall problem with convective boundary conditions. *Commun. Nonlinear Sci. Numer. Simulat.* 2011; **16**, 752-60.
- [13] SV Subhashini, N Samuel and I Pop. Double-diffusive convection from a permeable vertical surface under convective boundary condition. *Int. Commun. Heat Mass Tran.* 2011; **38**, 1183-8.
- [14] JH Merkin and I Pop. The forced convection flow of a uniform stream over a flat surface with a convective surface boundary condition. *Commun. Nonlinear Sci. Numer. Simulat.* 2011; **16**, 3602-9.
- [15] OD Makinde and A Aziz. Boundary layer flow of a nanofluid past a stretching sheet with a convective boundary condition. *Int. J. Therm. Sci.* 2011; **50**, 1326-32.
- [16] SJ Liao. Beyond perturbation: Introduction to the homotopy analysis method, London/Boca Raton (FL), Chapman & Hall, CRC Press, 2003.
- [17] SJ Liao. A new branch of solutions of boundary layer flows over an impermeable stretching plate. *Int. J. Heat Mass Tran.* 2005; **48**, 2529-39.
- [18] S Abbasbandy. The application of homotopy analysis method to nonlinear equations arising in heat transfer. *Phys. Lett. A* 2006; **360**, 109-13.
- [19] S Abbasbandy and T Hayat. On series solution of unsteady boundary layer equations in a special third grade fluid. *Commun. Nonlinear Sci. Numer. Simulat.* 2011; **16**, 3140-6.
- [20] R Ali and A Shahzad. MHD flow of a non-Newtonian Power law fluid over a vertical stretching sheet with the convective boundary condition. *Walailak J. Sci. & Tech.* 2013; **10**, 43-56.
- [21] T Hayat, M Khan and M Ayub. On the explicit analytic solution of an Oldroyd 6-constant fluid. *Int. J. Eng. Sci.* 2004; **42**, 123-35.
- [22] A Shahzad and R Ali. Approximate analytic solution for magneto-hydrodynamic flow of a non-Newtonian fluid over a vertical stretching sheet. *Can. J. Appl. Sci.* 2012; **2**, 202-15.
- [23] M Khan and J Farooq. On heat transfer analysis of a magnetohydrodynamic Sisko fluid through a porous medium. *J. Porous Med.* 2010; **13**, 287-94.
- [24] M Khan, S Munawar and S Abbasbandy. Steady flow and heat transfer of a Sisko fluid in annular pipe. *Int. J. Heat Mass Tran.* 2010; **53**, 1290-7.
- [25] T Hayat, M Farooq and Z Iqbal. Stretched flow of Casson fluid with variable thermal conductivity. *Walailak J. Sci. & Tech.* 2013; **10**, 181-90.